Article

Surfactant Bilayers Maintain Transmembrane Protein Activity

Gamal Rayan,[1] Vladimir Adrien,[1,2] Myriam Reffay,[1] Martin Picard,[2] Arnaud Ducruix,[2] Marc Schmutz,[3] Wladimir Urbach,[1,4,5,6] and Nicolas Taulier[4,5,6,*]

[1]Laboratoire de Physique Statistique de l'École Normale Supérieure, UPMC, Université Paris Diderot, CNRS, UMR 8550, Paris, France; [2]Laboratoire de Cristallographie et RMN Biologiques, Université Paris Descartes, CNRS, UMR 8015, Paris, France; [3]Institut Charles Sadron - UPR 022 – CNRS - Unistra, Strasbourg, France; [4]Sorbonnes Université Univ Paris 6, UMR 7371, UMR_S 1146, Laboratoire d'Imagerie Biomédicale, Paris, France; [5]CNRS, UMR 7371, Laboratoire d'Imagerie Biomédicale, Paris, France; and [6]INSERM, UMR_S 1146, Laboratoire d'Imagerie Biomédicale, Paris, France

ABSTRACT In vitro studies of membrane proteins are of interest only if their structure and function are significantly preserved. One approach is to insert them into the lipid bilayers of highly viscous cubic phases rendering the insertion and manipulation of proteins difficult. Less viscous lipid sponge phases are sometimes used, but their relatively narrow domain of existence can be easily disrupted by protein insertion. We present here a sponge phase consisting of nonionic surfactant bilayers. Its extended domain of existence and its low viscosity allow easy insertion and manipulation of membrane proteins. We show for the first time, to our knowledge, that transmembrane proteins, such as bacteriorhodopsin, sarcoplasmic reticulum Ca^{2+}ATPase (SERCA1a), and its associated enzymes, are fully active in a surfactant phase.

INTRODUCTION

Transmembrane proteins are involved in many important cellular processes, such as solute transport, signal transduction, and detoxification. In vivo, the cell membrane, mainly composed of lipids, provides the hydrophobic environment suitable for maintaining the membrane proteins properly folded and thus functional. Biophysical studies on membrane protein must therefore provide a mimetic environment allowing their manipulation in solution as well as maintaining the necessary hydrophobic properties found in vivo in phospholipid membranes. The use of lipidic mesophases (such as the cubic phase) has recently gained much popularity with particular emphasis in the membrane protein crystallization field (1,2). A mesophase is a liquid crystal phase (3), and the technique of protein crystallization using a mesophase has been named the in meso method (1,2,4,5). In 1996 the first reported crystallization of a membrane protein was that of bacteriorhodopsin in a lipidic cubic phase (6). Since then, numerous membrane protein structures crystallized in meso have been reported (2,5,7–16). In 2011 the number of membrane proteins structures determined by the in meso method and deposited in the Protein Data Bank (www.mpdb.tcd.ie) (17) stood at 79 (15), and it is increasing steadily (18–20). The Caffrey group has been particularly instrumental in advocating the use of mesophases for crystallizing membrane proteins (1,5,12–14,19,21), and has recently reported the crystallization of a transmembrane peptide in meso (22,23). However, to be of interest, the obtained protein crystal structure should be one of a protein that remains active and despite the successful use of the in meso crystallization method in membrane structural studies, some issues regarding its biological/physiological relevance were raised recently (24). In addition, a recent small angle x-ray scattering and optical absorption spectroscopy study has shown that bacteriorhodopsin (BR) inserted into a cubic monoolein (MO) phase was distorted to the point of being forced to lose its retinal, which was caused by the membrane-induced saddle splay (25). However, several studies have shown that lipidic cubic phases are indeed relevant. In 1995, Hochkoeppler et al. (26) had shown that the membrane proteins as well as the associated soluble proteins of a bacterial photosynthetic reaction center retained their activity inside a lipidic cubic phase. More recently, the Caffrey group has addressed these concerns (27) and has reported the activity of an integral membrane protein embedded in the bilayers of a lipidic cubic phase (28).

Although the majority of membrane proteins whose structures were solved, were crystallized in the lipidic cubic phase, an increasing number of structures were deduced in the lipidic sponge (or L_3) phase (1,8,10–12,29). Globally, the sponge phase may be viewed as a molten cubic phase. Locally, it mimics the lamellar (L_α) phase, i.e., a stack of membranes with a characteristic separating distance. From the topological point of view the L_3 phase is a bicontinuous mesophase consisting of a single curved bilayer that divides a three-dimensional space in two continuous interpenetrating but nonconnected spaces filled with aqueous solution (30). A practical advantage of the sponge phase is that its

Submitted December 12, 2013, and accepted for publication July 7, 2014.

*Correspondence: nicolas.taulier@upmc.fr

Myriam Reffay's present address is: Laboratoire Matière et Systèmes Complexes - UMR 7057, Université Paris Diderot, CNRS Paris, F-75251, France.

Editor: Andreas Engel.

0006-3495/14/09/1129/7 $2.00

http://dx.doi.org/10.1016/j.bpj.2014.07.016

viscosity is much lower than the viscosity of the cubic phase, as well as that of the lamellar phase, hence is easier to manipulate. Most cubic and L_3 phases are prepared from MO, a lipid that can form several phases in aqueous solution: lamellar, cubic, hexagonal, and fluid isotropic/inverse micellar (31–33). Addition of some polar cosurfactants to this binary system (i.e., MO/water) results in the formation of an L_3 phase (34,35). Unfortunately, this phase lies in a very narrow area of the phase diagram, regardless of the cosurfactant used. This limitation is a real problem as any addition to the system (e.g., introduction of a membrane protein) might be sufficient to shift the phase diagram away from its original position, leading to a possible loss of the L_3 phase. For instance, Conn and colleagues have demonstrated that the incorporation of the dopamine D2L receptor and BR within a cubic MO phase affected the structure of the phase, and this effect was dependent on the structure of the embedded protein (36,37).

Larger and more stable sponge phase domains can be reached by replacing lipids by nonionic surfactants (38). Indeed >20 years ago Strey and colleagues (39) demonstrated the existence of an L_3 phase in the binary system composed of pentaethylene glycol monododecyl ether ($C_{12}E_5$), a nonionic surfactant that is routinely used in membrane protein crystallization (40), and water. However this sponge phase exists only at temperatures higher than 50°C, and very high water contents (>99% wt.), which make this phase unsuitable for protein studies. Moreover, the addition of a large quantity of solubilized proteins to the previous water/$C_{12}E_5$ sponge phase would alter the phase if the additional detergent used to solubilize the proteins is not $C_{12}E_5$.

We have solved all these problems by adding *n*-octyl-β-D-glucopyranoside (β-OG) to the binary water/$C_{12}E_5$ system of Strey et al. (39). This cosurfactant, which is a nonionic detergent used in membrane protein studies (41), dramatically lowered the temperature boundary of the sponge phase in the phase diagram. To the best of our knowledge this is an unusual L_3 phase. The bilayers of the phase can be swollen by the addition of dodecane (42), and the intermembrane distance can be adjusted by varying the water content from 5 to 50 nm (43). Moreover, compared to the MO/polar solvent/water L_3 phase, the viscosity of the β-OG/$C_{12}E_5$/water L_3 phase is much lower, and contrary to what has been suggested recently (44), the phase exists in a wide region of the phase diagram as shown below.

In our previous studies (43,45), we showed that several membrane proteins (MexA, MexB, OprM, OmpA, and BR) and membrane peptides could be easily inserted into the bilayer of this sponge phase. Furthermore, we have verified for several transmembrane proteins that their native structure is retained in this L_3 phase. For the latter, we use the fact that L_3 phase is optically isotropic (unlike L_α) and transparent, thus amenable to spectroscopic studies. We have also shown that the addition of these membrane proteins did not affect the phase properties at least for concentrations lower than 60 μM (43). Moreover, we would like to point out that the insertion of membrane proteins into the phase would result in the addition of protein-bound lipids to the phase. This does not change the properties of the phase, as those lipids are tightly bound to proteins and can thus be considered as an integral component of the lipid-protein system. The fact that the addition of proteins and hence protein-bound lipids at concentrations as high as 60 μM did not alter the properties of the phase (43) further corroborates this point.

It is important to emphasize that in addition to membrane protein and peptide crystallization (1,5,10,11,22) lipidic sponge phases have been used in various applications such as in drug delivery (46,47), in the extraction of polycyclic aromatic hydrocarbons (48), in the studies of the lateral diffusion of membrane proteins and peptides (42,45), and the interactions between transmembrane proteins (43).

However, it is still a matter of debate if transmembrane proteins retain their activity when inserted into the bilayers of a surfactant sponge phase, as is the case for the lipidic cubic phase (28). In this article, we show that this is effectively the case for the transmembrane proteins BR and sarcoplasmic reticulum Ca^{2+} ATPase (SERCA1a). This believed novel fact adds further appeal to the surfactant sponge phase as a biomimetic medium.

MATERIALS AND METHODS

Materials

Sodium chloride, sodium phosphate monobasic and dibasic, and glycerol were purchased from Sigma-Aldrich (St. Louis, MO). These reagents were used to make the 100 mM NaCl, 50 mM sodium phosphate, 5% (v/v) glycerol, pH 7.5 buffer that was complemented with the desired detergent. SERCA1a was handled in a 100 mM KCl, 50 mM MOPS Tris, 5mM Mg, 1mM Ca^{2+}, pH 7.5 buffer also from Sigma-Aldrich.

Phosphoenolpyruvate (PEP), pyruvate kinase (PK), lactate dehydrogenase (LDH), nicotinamide adenine dinucleotide (NADH), and ATP (disodium salt) were purchased from Sigma-Aldrich.

The nonionic detergents β-OG and Pentaethylene glycol monododecyl ether ($C_{12}E_5$) were purchased from Affymetrix-Anatrace (Maumee, OH) and Nikko Chemicals (Tokyo, Japan), respectively.

C_{12}-FITC, a fluorescent probe, was obtained from Life Technologies-Invitrogen (Grand Island, NY).

Sample preparation

Samples were prepared by mixing the required amounts of surfactant ($C_{12}E_5$), cosurfactant (β-OG), and water (or buffer) into glass vials. The samples were vortexed, sonicated, and equilibrated at 20°C for several days before characterization of the resultant phases. Cosurfactants were dissolved in water (or buffer) at a stock concentration of 10% (w/v).

Freeze fracture electron microscopy (FFEM)

The microstructures of the samples were studied by FFEM. A drop of the liquid sample was placed between two small copper holders to form a sandwich, which was then quickly plunged into liquid nitrogen to freeze the sample. The copper holder, with the frozen sample, was transferred into a

homemade cryo fracture apparatus. The sample was fractured under high vacuum at −160°C and right away a thin layer of platinum (2 nm) was evaporated under a 45° angle and a thick carbon film (20 nm) was deposited at 90° to reinforce the replica. The sample was warmed to room temperature under a dry N_2 stream. The replicas were washed in $CHCl_3$ to remove any remaining component of the original sample. Finally, the resulting solid replica was collected on 400 mesh copper grids, and observed at 200 kV with a Tecnai G2 FEI transmission electron microscope (FEI France, Mérignac, France), the images were recorded with a slow scan EAGLE camera (FEI France, Mérignac, France).

Protein production, purification, and labeling with FITC

SERCA1a was prepared from rabbit fast-twitch skeletal muscle following the protocol described in (49). SERCA1a labeling was adapted from (50) with the following changes. SR vesicles were suspended to a concentration of 2 mg/ml into Tricine-Tris pH8 (100 mM), 0.3 M sucrose, 1 mM $MgCl_2$, 0.01 mM Ca^{2+}. Labeling was performed by incubating the latter with 0.2 mM FITC for 1 h. The reaction was stopped upon a 10× dilution into ice-cold, FITC-free labeling, buffer. Under such conditions, protein was labeled with a 1:1 efficiency.

Halobacter halobium cells were grown under illumination at 37°C in a liquid growth medium containing NaCl 4 M, $MgSO_4$ 150 mM, trisodium citrate 10 mM, KCl 30 mM, yeast extract 5 g/L, and peptone 5 g/L. Purple membrane was purified on a 30–40% (w/v) sucrose gradient (100,000 × *g* for 17 h). The membrane suspension was solubilized in Tris HCl 20mM, glycerol 5%, octylglucoside 0.9% for 48 h at 37°C. The volume for the solubilization was set to resuspend the membrane at a 1:5 (w/w) protein/detergent ratio. The concentration of solubilized BR was estimated using ε (570 nm) = 54,000 $M^{-1}cm^{-1}$. Solubilized BR was ultracentrifuged (100,000 × *g* for 20′) to get rid of lipids and insolubilized proteins.

Protein insertion in the phase

For all the proteins investigated, insertion was performed by simply adding a required volume of detergent-solubilized protein into the surfactant, water, cosurfactant system, making sure that the required surfactant/cosurfactant ratio was maintained.

Protein activity in the phase

BR activity measurements: photocycle measurements were performed with a pump-probe spectrophotometer (51) in which the probe and pump ashes are respectively provided by a Panther Optical Parametric Oscillator (Continuum France S.A.S., Villebon sur Yvette, France) and a Brilliant frequency-doubled Nd:Yag laser (Quantel, France, Les Ulis, France). The kinetics of the absorption changes associated with the rise and decay of intermediates during the photocycle were recorded at 415 nm from 5 ns to 100 ms after a 5 ns actinic flash.

ATPase activity measurements

Spectrophotometric measurements of ATP hydrolysis by the Ca^{2+}-ATPase were performed with an ATP-regenerating coupled enzyme assay originally described by Pullman and co-workers (52) and subsequently adapted (53,54). We describe this measurement in more detail in the paragraph Results and Discussion. The reaction was performed in 100 μL of a medium containing 50 mM Tes-Tris, pH 7.0, 50 mM KNO_3, 7 mM $MgCl_2$, 1 mM PEP, 0.1 mg/ml PK, 0.1 mg/ml LDH, an initial concentration of ~0.3 mM NADH, 3–6 μg/ml of purified Ca^{2+}-ATPase and 0.1 mM total $CaCl_2$. The reaction was monitored through the variation of absorption at a wavelength of 340 nm using a Biochrom Libra S22 spectrophotometer (Biochrom, Cambridge, UK).

RESULTS AND DISCUSSION

Characterization of the L_3 phase

We checked that throughout the black line, drawn on the diagram of Fig. 1, the L_3 phase exists from 6 to 30°C, a temperature range more suitable for membrane protein studies than the $C_{12}E_5$/water system. The boundaries between the L_3 phase and the L_α phase can easily be detected optically, as the L_α phase is birefringent, whereas the sponge phase is isotropic. Moreover, the use of fluorescence recovery after pattern photobleaching (FRAPP) enables us to discern the boundaries of the two isotropic phases because the lateral diffusion of a fluorescent probe will vary significantly from one phase to another. The precision of the drawn boundaries in the diagram does not exceed 0.002 M.

Protein insertion into the surfactant bilayers of a sponge phase

First of all, we have checked that both proteins are effectively embedded into the bilayers of the β-OG/$C_{12}E_5$/water sponge phase by performing FRAPP. For each protein we have observed a single diffusion coefficient (D_{ATPase} = 1.7 ± 0.1 $\mu m/s^2$ and D_{BR} = 1.2 ± 0.2 $\mu m/s^2$) (Fig. 2) whose value was indicative of a macromolecule diffusing in the bilayers of a sponge phase (42,45).

The fact that the proteins are inserted into the bilayers was further confirmed by freeze fracture electron microscopy (Fig. 3).

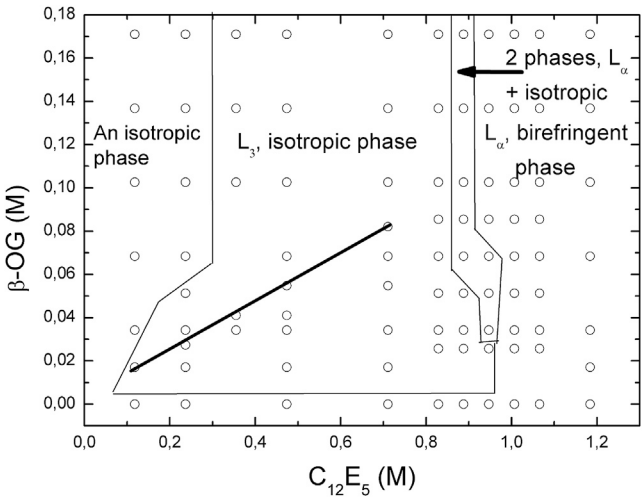

FIGURE 1 Partial phase diagrams of the ternary systems consisting of $C_{12}E_5$, water, and β-OG as cosurfactant. Each symbol corresponds to an experimental sample that was investigated at 20°C. The lines drawn on the diagram represent approximate boundaries between the phases. The black line in the L_3 region of the diagram corresponds to the dilution line that was investigated with the following methods; small angle x-ray scattering, small angle neutron scattering, FFEM, and FRAPP. Throughout this black line the L_3 phase exists from 6 to 30°C.

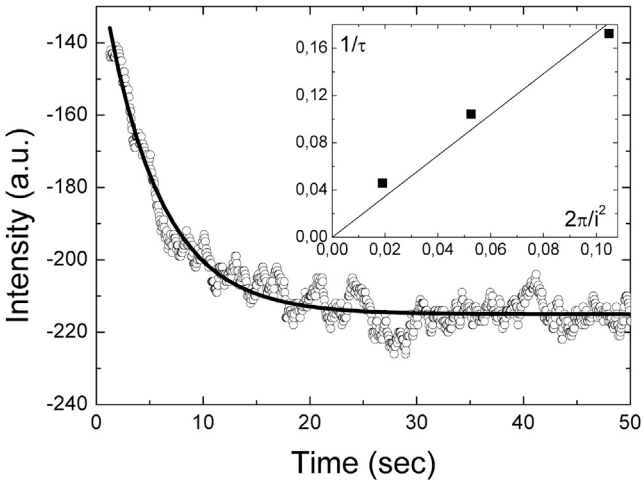

FIGURE 2 Typical decrease of the FRAPP fringes contrast as a function of time (here for SERCA1a in L_3). From the fit of this curve (measured at an interfringe distance i = 19.4 μm) we obtain a characteristic decay time $\tau = 5.2$ s, which corresponds to a D value of 1.7 $\pm$ 0.1 $\mu m/s^2$. In the inset, we present the variation of $1/\tau$ as a function of $(i/2\pi)^2$. The linear behavior indicates the Brownian motion of the protein embedded in the bilayers of L_3 phase and the slope of the linear fit leads to the self-diffusion coefficient of the protein.

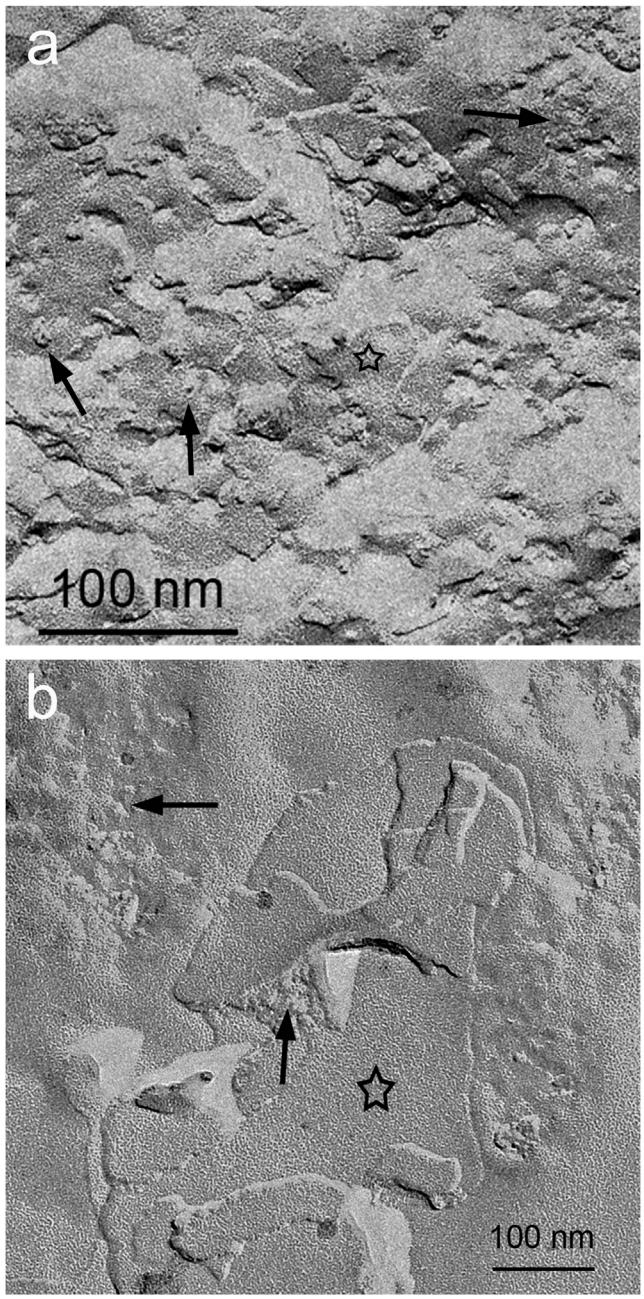

FIGURE 3 Freeze fracture electron microscopy of the L_3 containing (*a*) SERCA1a at 2.5 μM and (*b*) BR at 5.0 μM. The image represents the midplane of the bilayers of the sponge phase and the spots pointed by the arrows represent the replica of SERCA and BR proteins embedded in the bilayer. The stars point out to the region of the phase devoid of proteins.

BR activity

We have already observed that BR keeps its overall fold after being incorporated into the L_3 phase, as judged from its absorbance spectrum (Fig. S1 in the Supporting Material). It exhibits absorbance maxima at 280 nm and at 554 nm, a specific signature of the presence of retinal, a cofactor covalently bound to the protein. When the protein denatures the retinal signal is lost. The functionality of BR can be monitored from the analysis of the photocycle it undergoes upon illumination. BR samples prepared in various environments (purple membrane, β-OG micelles and L_3 phase) were excited at 640 nm by a 5 ns laser flash. Flash-induced absorption changes were monitored with a time resolution of 5 ns at various wavelengths. The kinetics of the absorption changes reflect the appearance and disappearance of the steps undergone by the protein during its transport cycle. Each of these steps has specific wavelength maxima: for instance, 415 nm is a wavelength specific of a key step: the M_1–M_2 transconformation where the increase of the absorbance is due to the deprotonating of the Schiff's base.

To unambiguously show that the L_3 phase does not affect the activity of the BR, we have focused on the building of the M intermediate state. Indeed, this step corresponds to the largest conformational change performed by the protein, leading to the opening of cytoplasmic channel and hence to the directionality of proton pumping. It is hence a relevant indicator of the overall activity of the protein. As can be seen in the case of the control where the protein is located in its native membrane (Fig. 4), the time resolved absorption spectrum is bell-shaped: the absorption maximum is attained and then the protein relaxes down to its initial level. We observe that BR also performs a photocycle when it is reconstituted in the L_3 phase (Fig. 4): the absorption maximum is reached in ~20 μs, i.e., significantly faster than in a membrane, and then relaxes back to its initial level, which is an unambiguous sign that the protein undergoes a full, genuine cycle. The exact same trend is observed when the protein is in detergent/β-OG micelles (Fig. 4). The faster

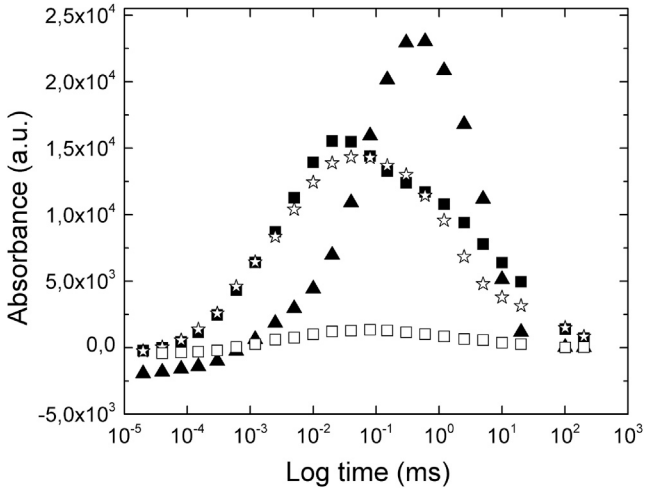

FIGURE 4 Time-resolved absorption of BR at 415 nm dissolved in the purple membrane (▲); β-OG micelles (☆); the L_3 phase (C_{BR} =2.1 μM) (■); the solution mimicking the intermembrane liquid space (C_{BR} = 0.1 μM) (□), see Results and Discussion.

rise of the M intermediates in the presence of detergent or upon reconstitution into the L_3 phase is in agreement with literature: it has been shown that the M_1-M_2 step is accelerated in detergent compared to what is observed in membrane (55). A tentative explanation is that the lateral pressure induced by the lipidic membrane on the protein is relaxed when the protein is solubilized and that this flexibility makes it easier for the protein to undergo its large conformational change. The same flexibility would be maintained in the L_3 phase.

One can still argue that the BR embedded in bilayers is inactive and that the observed BR activity is caused by small amounts of protein located in the liquid solution between the bilayers. We refuted this hypothesis by performing FRAPP experiments. Indeed, FRAPP should provide diffusion coefficients of slowly diffusing species, embedded into the surfactant bilayers, and rapidly diffusing species, located in the aqueous solvent between bilayers. Our FRAPP measurements showed only one, slowly diffusing, species corresponding to that of the bilayer-embedded protein. This however did not rule out the fact that tiny amounts of BR, undetectable by FRAPP, could still be solubilized in the aqueous solution and that the solubilized amount could be sufficient to produce the observed spectra. Thus, to mimic the activity of potential BR species dissolved in the solution located between the bilayers of the L_3 phase, we have solubilized BR in an aqueous solution of β-OG/$C_{12}E_5$ (both surfactants at a concentration below their respective critical micellar concentration values).The highest BR concentration undetectable by FRAPP was 0.1 μM, thus corresponding to the maximal amount of hypothetical residual protein inserted between bilayers. The observed activity is significantly lower (Fig. 4) than that observed when the BR, at a concentration of 2.1 μM, is dissolved in the sponge phase. This confirms that activity observed in phase L_3 is due to the BR incorporated into surfactant bilayers of L_3 phase.

SERCA1a activity

SERCA1a is a well-known membrane protein paradigm of the P-type ATPases. Its catalytic activity has been studied extensively from both functional and structural points of view (56,57). Of particular relevance to this work is the fact that this enzyme is known to be exceedingly sensitive to the particular detergent used to maintain it in solution (58). We then investigated the effect of the insertion of SERCA1a in the sponge phase by use of a coupled enzyme assay where, as the enzyme hydrolyses ATP and produces a molecule of ADP, PK catalyzes the dephosphorylation of PEP, leading to a molecule of pyruvate while, at the same time, the ADP molecule is reconverted to ATP. This reaction (so-called ATP regenerating system) allows to keep the concentration of ATP constant in the medium. In turn, the pyruvate formed is reduced to lactate by LDH and one molecule of NADH is oxidized into NAD+. Monitoring the decrease of the optical density at 340 nm, wavelength at which NADH absorbs, hence makes it possible to estimate the decrease in the concentration of NADH as a function of time, a value that is stoichiometrically related to ATP hydrolysis. The rate of hydrolysis is standardized to the quantity of proteins and is therefore expressed in micromole ATP hydrolyzed per milligram of protein per minute. We have reconstituted the SERCA1a into a sponge phase consisting of $C_{12}E_5$, β-OG, and MOPS-Tris buffer (see Materials and Methods). After the protein was solubilized either with β-OG or $C_{12}E_5$, the cognate detergent was added to reach a $C_{12}E_5$/β-OG ratio (w/w) consistent with the formation of an L_3 phase.

The latter detergent mixture was hydrated with a buffer containing the various enzymes necessary to perform a coupled-enzyme assay with proteins incorporated in an L_3 phase. The activity assay was carried out with an enzyme concentration equal to that used for the BR activity assay described previously. Here, we show that the ATPase activity for the protein incorporated into an L_3 phase is equal to 2.5 μmol mg^{-1} min^{-1}, a value in the same order of magnitude as that reported in $C_{12}E_8$, (octaethylene glycol monododecyl ether), a detergent known to be the most efficient at keeping the protein active in solution (53) (Fig. 5). Indeed, the activity of SERCA1a was previously shown to be in the range of 4–6 μmol /mg/min. Conversely, we observe the previously known fact that the protein activity is poorly maintained in the presence of β-OG (58).

In conclusion, we have shown for the first time, to our knowledge, that membrane proteins are active in surfactant bilayers. The L_3 phase, obtained by the addition of $C_{12}E_5$ and 10% of β-OG to buffer/water, is a convenient medium for incorporating membrane proteins into a biomimetic environment that makes it possible to endeavor into the investigation of various biophysical and biochemical

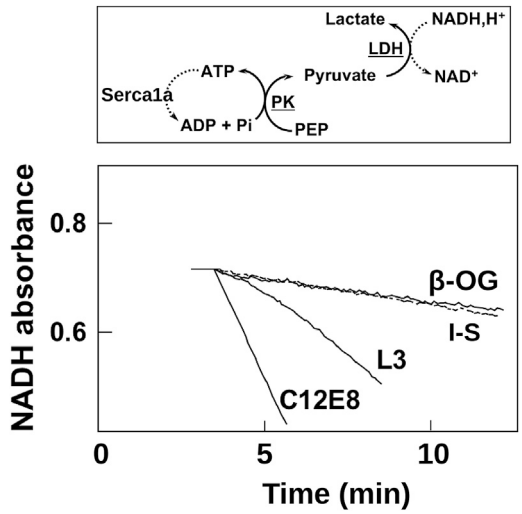

FIGURE 5 Enzymatic activity of the SERCA1a reconstituted in various environments. The end product of this coupled-enzyme assay is the oxidation of NADH to NAD^+, which is seen as the decrease in absorption at 340 nm (the *top panel*). In the bottom panel the activity of the enzyme in the L_3 phase is compared to its activity in micellar solutions of either β-OG (*low activity*), $C_{12}E_8$ (*high activity*), or in a medium mimicking the L_3 intermembrane space (I-S, *dotted line*, *low activity*). The latter measurement has been performed at an enzyme concentration of 0.1 μM corresponding to the threshold detection by FRAPP. All other measurements have been performed at 1 μM. ATP: adenosine triphosphate. ADP: adenosine diphosphate. NAD: nicotinamide adenine dinucleotide. PK: pyruvate kinase. PEP: phosphoenolpyruvic acid.

parameters, such as the measurement of lateral diffusion (42,43,45); determination of interaction stoichiometry (43); or protein crystallization, while preserving the membrane protein activity, even though β-OG is a harsh surfactant when compared to milder surfactants such as DDM, Cymal-4, and Cymal-5. In addition, our approach remains valid by replacing β-OG by milder surfactants that do not destabilize the sponge phase structure.

SUPPORTING MATERIAL

One figure is available at http://www.biophysj.org/biophysj/supplemental/S0006-3495(14)00734-6.

We gratefully acknowledge Fabrice Rappaport for bacteriorhodopsin activity measurements.

We thank the Agence Nationale de la Recherche (ANR) for the funds provided for this study (Project ASSEMBLY, Grant ANR-12-BSV8-0010).

REFERENCES

1. Caffrey, M. 2009. Crystallizing membrane proteins for structure determination: use of lipidic mesophases. *Annu. Rev. Biophys.* 38:29–51.
2. Caffrey, M. 2011. Crystallizing membrane proteins for structure-function studies using lipidic mesophases. *Biochem. Soc. Trans.* 39:725–732.
3. Hyde, S. T. 2001. Identification of lyotropic liquid crystalline mesophases. *In* Handbook of Applied Surface and Colloid Chemistry. K. Holmberg, editor. John Wiley & Sons, West Sussex, pp. 299–332.
4. Caffrey, M. 2005. Membrane protein crystallization in lipidic bicontinuous liquid crystals. *In* Bicontinuous Liquid Crystals. M. L. Lynch and P. T. Spicer, editors. CRC Press, Boca Raton, FL, pp. 307–319.
5. Caffrey, M., and V. Cherezov. 2009. Crystallizing membrane proteins using lipidic mesophases. *Nat. Protoc.* 4:706–731.
6. Landau, E. M., and J. P. Rosenbusch. 1996. Lipidic cubic phases: a novel concept for the crystallization of membrane proteins. *Proc. Natl. Acad. Sci. USA.* 93:14532–14535.
7. Pebay-Peyroula, E., G. Rummel, …, E. M. Landau. 1997. X-ray structure of bacteriorhodopsin at 2.5 angstroms from microcrystals grown in lipidic cubic phases. *Science.* 277:1676–1681.
8. Johansson, L. C., A. B. Wöhri, …, R. Neutze. 2009. Membrane protein crystallization from lipidic phases. *Curr. Opin. Struct. Biol.* 19: 372–378.
9. Nollert, P. 2004. Lipidic cubic phases as matrices for membrane protein crystallization. *Methods.* 34:348–353.
10. Wöhri, A. B., L. C. Johansson, …, R. Neutze. 2008. A lipidic-sponge phase screen for membrane protein crystallization. *Structure.* 16:1003–1009.
11. Wadsten, P., A. B. Wöhri, …, S. Engström. 2006. Lipidic sponge phase crystallization of membrane proteins. *J. Mol. Biol.* 364:44–53.
12. Cherezov, V., J. Clogston, …, M. Caffrey. 2006. Room to move: crystallizing membrane proteins in swollen lipidic mesophases. *J. Mol. Biol.* 357:1605–1618.
13. Caffrey, M. 2003. Membrane protein crystallization. *J. Struct. Biol.* 142:108–132.
14. Caffrey, M. 2000. A lipid's eye view of membrane protein crystallization in mesophases. *Curr. Opin. Struct. Biol.* 10:486–497.
15. Cherezov, V. 2011. Lipidic cubic phase technologies for membrane protein structural studies. *Curr. Opin. Struct. Biol.* 21:559–566.
16. Tiefenbrunn, T., W. Liu, …, V. Cherezov. 2011. High resolution structure of the ba3 cytochrome *c* oxidase from *Thermus thermophilus* in a lipidic environment. *PLoS ONE.* 6:e22348.
17. Raman, P., V. Cherezov, and M. Caffrey. 2006. The Membrane Protein Data Bank. *Cell. Mol. Life Sci.* 63:36–51.
18. Kubicek, J., R. Schlesinger, …, J. Labahn. 2012. Controlled in meso phase crystallization—a method for the structural investigation of membrane proteins. *PLoS ONE.* 7:e35458.
19. Caffrey, M., D. Li, and A. Dukkipati. 2012. Membrane protein structure determination using crystallography and lipidic mesophases: recent advances and successes. *Biochemistry.* 51:6266–6288.
20. Li, D., S. T. A. Shah, and M. Caffrey. 2013. Host lipid and temperature as important screening variables for crystallizing integral membrane proteins in lipidic mesophases. Trials with diacylglycerol kinase. *Cryst. Growth Des.* 13:2846–2857.
21. Ai, X., and M. Caffrey. 2000. Membrane protein crystallization in lipidic mesophases: detergent effects. *Biophys. J.* 79:394–405.
22. Höfer, N., D. Aragão, and M. Caffrey. 2010. Crystallizing transmembrane peptides in lipidic mesophases. *Biophys. J.* 99:L23–L25.
23. Höfer, N., D. Aragão, …, M. Caffrey. 2011. Membrane protein crystallization in lipidic mesophases. Hosting lipid affects on the crystallization and structure of a transmembrane peptide. *Cryst. Growth Des.* 11:1182–1192.
24. Separovic, F., J. A. Killian, …, T. A. Cross. 2011. Modeling the membrane environment for membrane proteins. *Biophys. J.* 100:2073–2074, author reply 2075.
25. Kulkarni, V. C., A. M. Seddon, …, R. H. Templer. 2010. Evidence that membrane curvature distorts the tertiary structure of bacteriorhodopsin. *Soft Matter.* 6:4339–4341.
26. Hochkoeppler, A., E. M. Landau, …, P. L. Luisi. 1995. Photochemistry of a photosynthetic reaction center immobilized in lipidic cubic phases. *Biotechnol. Bioeng.* 46:93–98.
27. Hofer, N., D. Aragao, and M. Caffrey. 2011. The lipidic cubic phase as a membrane mimetic. *Biophys. J.* 100:2075.

28. Li, D., and M. Caffrey. 2011. Lipid cubic phase as a membrane mimetic for integral membrane protein enzymes. *Proc. Natl. Acad. Sci. USA.* 108:8639–8644.

29. Johansson, L. C., D. Arnlund, …, R. Neutze. 2012. Lipidic phase membrane protein serial femtosecond crystallography. *Nat. Methods.* 9:263–265.

30. Beck, R., and H. Hoffmann. 2005. Novel L_3 phases and their macroscopic properties. *In* Bicontinuous Liquid Crystals. M. L. Lynch and P. T. Spicer, editors. CRC Press, Boca Raton, FL, pp. 131–167.

31. Briggs, J., H. Chung, and M. Caffrey. 1996. The temperature-composition phase diagram and mesophase structure characterization of the monoolein/water system. *J. Phys. II France.* 6:723–751.

32. Kulkarni, C. V., W. Wachter, …, S. Ahualli. 2011. Monoolein: a magic lipid? *Phys. Chem. Chem. Phys.* 13:3004–3021.

33. Qiu, H., and M. Caffrey. 2000. The phase diagram of the monoolein/water system: metastability and equilibrium aspects. *Biomaterials.* 21:223–234.

34. Engstrom, S., K. Alfons, …, H. Ljusberg-Wahren. 1998. Solvent-induced sponge (L3) phases in the solvent-monoolein-water system. *Prog. Colloid Polym. Sci.* 108:93–98.

35. Wadsten-Hindrichsen, P., J. Bender, …, S. Engström. 2007. Aqueous self-assembly of phytantriol in ternary systems: effect of monoolein, distearoylphosphatidylglycerol and three water-miscible solvents. *J. Colloid Interface Sci.* 315:701–713.

36. Conn, C. E., C. Darmanin, …, C. J. Drummond. 2010. Incorporation of the dopamine D2L receptor and bacteriorhodopsin within bicontinuous cubic lipid phases. 1. Relevance to in meso crystallization of integral membrane proteins in monoolein systems. *Soft Matter.* 6:4828–4837.

37. Conn, C. E., C. Darmanin, …, C. J. Drummond. 2010. Incorporation of the dopamine D2L receptor and bacteriorhodopsin within bicontinuous cubic lipid phases. 2. Relevance to in meso crystallization of integral membrane proteins in novel lipid systems. *Soft Matter.* 6:4838–4846.

38. Zapf, A., U. Hornfeck, …, H. Hoffmann. 2001. Investigation of the L3 phase in systems containing calcium dodecyl sulfate, alcohol, and water. *Langmuir.* 17:6113–6118.

39. Strey, R., R. Schomacker, …, U. Olsson. 1990. Dilute lamellar and L_3 phases in the binary water-$C_{12}E_{15}$ system. *J. Chem. Soc., Faraday Trans.* 86:2253–2261.

40. Welling, G. W., Y. Hiemstra, …, S. Welling-Wester. 1992. Comparison of detergents for extraction and ion-exchange high-performance liquid chromatography of Sendai virus membrane proteins. *J. Chromatogr. A.* 599:157–162.

41. Privé, G. G. 2007. Detergents for the stabilization and crystallization of membrane proteins. *Methods.* 41:388–397.

42. Gambin, Y., M. Reffay, …, W. Urbach. 2010. Variation of the lateral mobility of transmembrane peptides with hydrophobic mismatch. *J. Phys. Chem. B.* 114:3559–3566.

43. Reffay, M., Y. Gambin, …, W. Urbach. 2009. Tracking membrane protein association in model membranes. *PLoS ONE.* 4:e5035.

44. Lepzelter, D., and M. Zaman. 2012. Subdiffusion of proteins and oligomers on membranes. *J. Chem. Phys.* 137:175102.

45. Gambin, Y., R. Lopez-Esparza, …, W. Urbach. 2006. Lateral mobility of proteins in liquid membranes revisited. *Proc. Natl. Acad. Sci. USA.* 103:2098–2102.

46. Alfons, K., and S. Engstrom. 1998. Drug compatibility with the sponge phases formed in monoolein, water, and propylene glycol or poly(ethylene glycol). *J. Pharm. Sci.* 87:1527–1530.

47. Merclin, N., J. Bender, …, S. Engström. 2004. Transdermal delivery from a lipid sponge phase—iontophoretic and passive transport in vitro of 5-aminolevulinic acid and its methyl ester. *J. Control. Release.* 100:191–198.

48. Hung, K. C., and B. H. Chen. 2007. Application of L3 Sponge Phase in Extraction of Polycyclic Aromatic Hydrocarbons. *AIChE J.* 53:1450–1459.

49. Lüdi, H., and W. Hasselbach. 1985. Preparation of a highly concentrated, completely monomeric, active sarcoplasmic reticulum Ca2+-ATPase. *Biochim. Biophys. Acta.* 821:137–141.

50. Champeil, P., S. Riollet, …, D. B. McIntosh. 1988. ATP regulation of sarcoplasmic reticulum Ca2+-ATPase. Metal-free ATP and 8-bromo-ATP bind with high affinity to the catalytic site of phosphorylated ATPase and accelerate dephosphorylation. *J. Biol. Chem.* 263:12288–12294.

51. Béal, D., F. Rappaport, and P. Joliot. 1999. A new high-sensitivity 10-ns time-resolution spectrophotometric technique adapted to in vivo analysis of the photosynthetic apparatus. *Rev. Sci. Instrum.* 70:202–207.

52. Pullman, M. E., H. S. Penefsky, …, E. Racker. 1960. Partial resolution of the enzymes catalyzing oxidative phosphorylation. I. Purification and properties of soluble dinitrophenol-stimulated adenosine triphosphatase. *J. Biol. Chem.* 235:3322–3329.

53. Lund, S., S. Orlowski, …, J. V. Møller. 1989. Detergent structure and associated lipid as determinants in the stabilization of solubilized Ca2+-ATPase from sarcoplasmic reticulum. *J. Biol. Chem.* 264: 4907–4915.

54. Møller, J. V., K. E. Lind, and J. P. Andersen. 1980. Enzyme kinetics and substrate stabilization of detergent-solubilized and membraneous (Ca2+ + Mg2+)-activated ATPase from sarcoplasmic reticulum. Effect of protein-protein interactions. *J. Biol. Chem.* 255:1912–1920.

55. Milder, S. J., T. E. Thorgeirsson, …, D. S. Kliger. 1991. Effects of detergent environments on the photocycle of purified monomeric bacteriorhodopsin. *Biochemistry.* 30:1751–1761.

56. Møller, J. V., C. Olesen, …, P. Nissen. 2005. The structural basis for coupling of Ca2+ transport to ATP hydrolysis by the sarcoplasmic reticulum Ca2+-ATPase. *J. Bioenerg. Biomembr.* 37:359–364.

57. Toyoshima, C. 2008. Structural aspects of ion pumping by Ca2+-ATPase of sarcoplasmic reticulum. *Arch. Biochem. Biophys.* 476:3–11.

58. le Maire, M., P. Champeil, and J. V. Moller. 2000. Interaction of membrane proteins and lipids with solubilizing detergents. *Biochim. Biophys. Acta.* 1508:86–111.

Surfactant Bilayers Maintain Transmembrane Protein Activity

G. Rayan,[1] V. Adrien,[1,2] M. Reffay,[1] M. Picard,[2] A. Ducruix,[2] M. Schmutz,[3] W. Urbach,[1,4,5,6] and N. Taulier[4,5,6,*]

[1]Laboratoire de Physique Statistique de l'École Normale Supérieure, UPMC, Université Paris Diderot, CNRS, Paris, France; [2]Laboratoire de Cristallographie et RMN Biologiques, Université Paris Descartes, CNRS, Paris, France; [3]Institut Charles Sadron - UPR 022 – CNRS - Unistra, Strasbourg, France; [4]Sorbonnes Université Univ Paris 6, UMR 7371, UMR_S 1146, Laboratoire d'Imagerie Biomédicale, Paris, France; [5]CNRS, UMR 7371, Laboratoire d'Imagerie Biomédicale, Paris, France; and [6]INSERM, UMR_S 1146, Laboratoire d'Imagerie Biomédicale, Paris, France

SUPPORTING MATERIALS

Fig. S1. UV-absorption spectra of bacteriorohodopsin in the purple membrane (blue line), in β- OG micelles (green line), in the L_3 phase (black line), and the denatured protein (light-blue line).

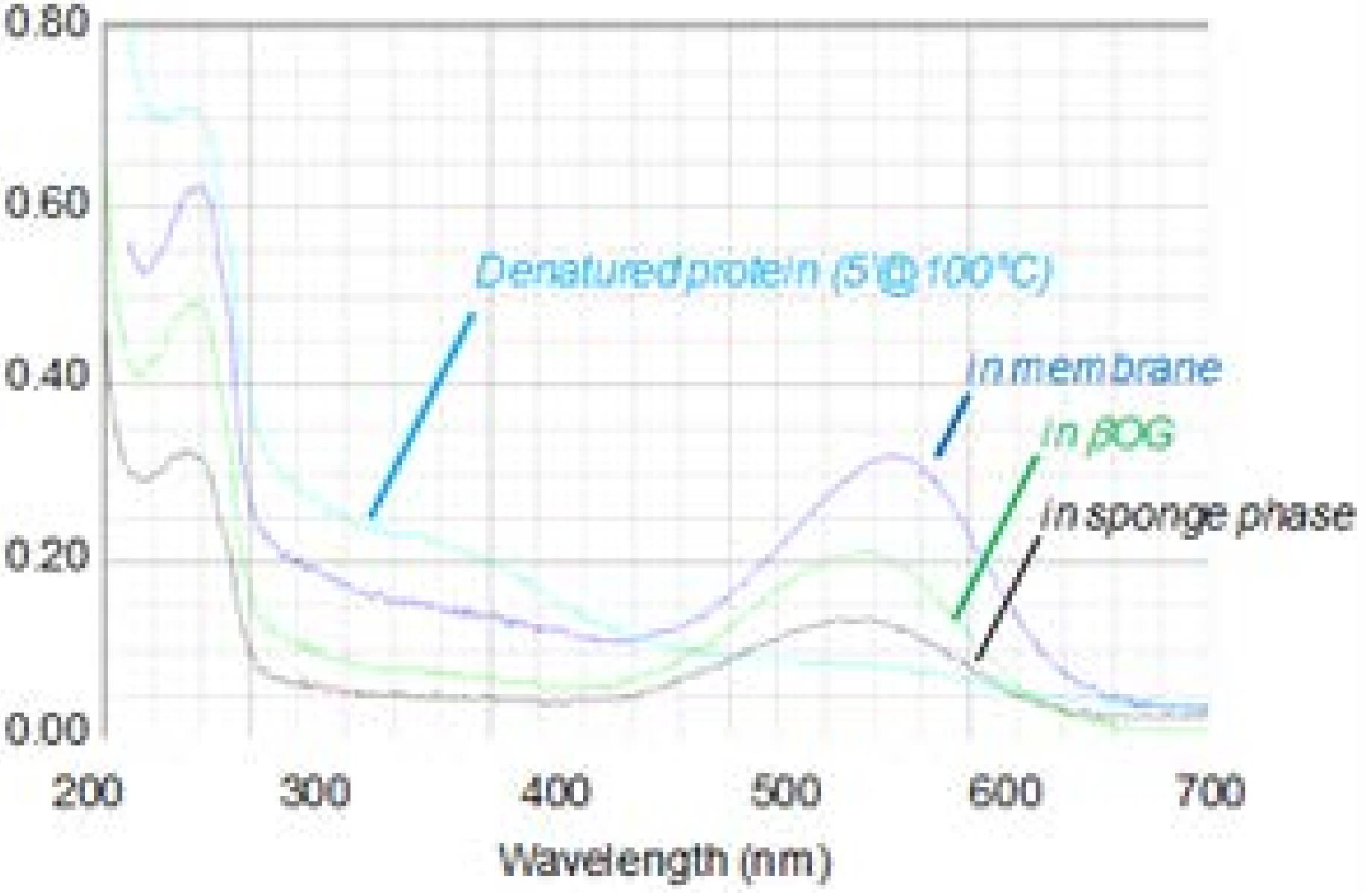
0.80
0.60
0.40
0.20
0.00
200
300
400
500
600
700
Wavelength (nm)
Denatured protein (5' @ 100°C)
In membrane
In βOG
In sponge phase